Available online at www.sciencedirect.com

ScienceDirect

Energy Procedia 44 (2014) 96 – 104

Energy Procedia

E-MRS Spring Meeting 2013 Symposium D - Advanced Inorganic Materials and Structures for Photovoltaics, 27-31 May 2013, Strasbourg, France

Co-evaporated Tin Sulfide thin films on bare and Mo-coated glass substrates as photovoltaic absorber layers

V. Robles[a]*, J.F. Trigo[a], C. Guillén[a], J. Herrero[a]

[a]*CIEMAT , Department of Energy, Avda. Complutense 40 Ed.42, Madrid 28040, Spain*

Abstract

This work has been focused on the synthesis by co-evaporation on bare and Mo-coated glass substrates of tin sulfide films with thicknesses in the 700-1200 nm range for use as absorber layers, with a substrate temperature at 350 °C and a sulfur partial pressure of 1-2*10^{-3} Pa. After evaporation, the samples were heated at 500 °C under Ar atmosphere. The evolution of the morphological, structural, chemical and optical properties of the samples deposited on bare or Mo-coated glass substrates has been analyzed as a function of the thickness, before and after annealing. For the samples grown on bare glass, some phase mixing has been observed by X-ray diffraction (XRD). Samples with reduced thickness preferably crystallize in the SnS phase, whereas thicker layers crystallize in the Sn_2S_3 phase. Otherwise, the Mo-coated glass substrate favors the crystallinity in the phase SnS preferably. Scanning electron microscope (SEM) shows thin films with homogeneous and uniform surface. All samples were characterized by reflectance (R) and transmittance (T) measurements in the wavelength range 300-1500 nm, showing an increase of the maxima of reflectance when the films are obtained on bare glass and after annealing. The energy band gap values, calculated from optical measurements of T and R, are between 1.14-1.20 eV, being suitable for absorbers layers in photovoltaic applications.

Keywords: film thickness, substrate temperature, annealing temperature, X-ray diffraction, termography, reflectance, band gap energy.

1. Introduction

Tin sulfides (Sn_xS_y) are IV-VI chalcogenide semiconductor materials which have reached great interest because

* Corresponding author. Tel.: +34-91-346-6679; fax: +34-91-346-6037.
E-mail address: victor.robles@ciemat.es

doi:10.1016/j.egypro.2013.12.014

they are made up of cheap and non-toxic elements, and also because depending on their stoichiometry (SnS, SnS_2 and Sn_2S_3) they can be used as absorbent or window materials in photovoltaic applications, being a potential substitute for other chalcogenides such as CdS, CdTe, CIS or CIGS [1, 2]. SnS presents an orthorhombic structure [3] GeS type [4] with the following lattice parameters a= 4.329 Å , b= 11.193 Å and c= 3.984 Å [5], it is usually a p-type semiconductor with a band gap around 1,3 eV [6], comprised between 1.12 eV and 1.43 eV, values that correspond to the absorber materials Si and GaAs [7] , and an absorption coefficient above 10^4 cm^{-1} [8], in the same order than for other chalcogenide materials like CdTe or CIS [9]. SnS_2 has a hexagonal [10] structure CdI_2 type [11], it can be used as window layer due to having energy band gap in the range 2.12-2.44 eV and with a n-type electrical conductivity [12]. Sn_2S_3 is classified as a mixed valence compound with semiconductor behaviour [13], that crystallizes in orthorhombic structure with lattice parameters a= 8.884 Å, b= 14.02 Å and c= 3.747 Å, and its energy band gap varies from 0.94 eV to 2.2 eV [14]. The combination of these phases allows to obtain devices such as diodes [12].

Tin sulfide thin films have been studied and prepared by other authors using different techniques such as multilayer-based solid-state reaction [15], spray pyrolysis [3, 6, 8,], constant-current electro-deposition [16], chemical bath deposition [17], radiofrequency sputtering [18], chemical vapour deposition [12, 13], sulfurization of metallic precursors [1, 19], dip deposition [11], vacuum thermal evaporation [2, 20], successive ionic layer adsorption and reaction (SILAR) [10], electrochemical deposition [21].

In this work, we have prepared tin sulfide thin films by co-evaporation on bare or Mo-coated soda-lime glass substrates, by the same procedure already reported by us [22] and also described by others authors [9, 23] . We have increased the deposition time of the co-evaporation process, to obtain tin sulfide thin films with thicknesses greater than 700 nm, in order to achieve layers with low transmittance as used in photovoltaic applications as absorbent material. Furthermore, preparation of tin sulfide thin films on Mo-coated glass substrate is investigated for possible manufacturing of photovoltaics heterojunctions in the same configuration that is commonly used for the CIS-based devices. The structural, morphological, chemical and optical properties have been analyzed by X-ray diffraction (XRD), energy dispersive analysis of X-rays (EDAX), scanning electron microscope (SEM) and optical measurements to determinate the influence of the film thickness, the substrate (bare or Mo-coated glass substrate) and the subsequent annealing.

2. Experimental details

Tin sulfide thin films were grown by co-evaporation of the precursor species on bare and Mo-coated soda-lime glass substrates. The deposition system is constituted by the evaporation chamber connected to a vacuum system; two sources, corresponding to evaporation of S and Sn respectively and a thickness monitor with a quartz sensor [22]. The parameters that have been controlled in the growth process were the deposition time and the glass substrate temperature at 350 ºC. Tin source temperature was optimized at 1200 °C for a constant growth of thin films and to obtain samples with thicknesses within a range between 700-1200 nm, maintaining constant sulfur partial pressure in a range of $1\text{-}2*10^{-3}$ Pa. Post-deposition annealing of the samples has been performed in a tubular furnace at 500 ºC during 30 min with flowing Ar.

The structure of the samples has been analyzed by XRD using the nickel-filtered *Ka*1 emission line of copper (λ= 1.5405 Å), in a Philips X'pert instrument. Film thickness was determined by profilometry using a DEKTAK 3030 profiler. Infrared thermography has been carried out by Testo 880 thermographic camera. Chemical analysis has been accomplished by EDAX with a JEOL 6400. Surface morphology has been analyzed by a JSM-6400 Scanning Electron Microscope (SEM). Optical measurements of the layers have been carried out with unpolarized light in the wavelength range from 300 to 1500 nm, with a double beam spectrophotometer Perkin-Elmer Lambda 9 including an integrating sphere to measure total and diffuse reflection as well as total transmission. The absorption coefficient (α) was calculated as a function of the photon energy from transmittance (T), reflectance (R), and the thickness values (t), and it allowed the determination of the band gap energy values.

3. Results and discussion

Figure 1 a-b shows the XRD diffractograms for the samples obtained on bare glass substrates with thicknesses of 700 and 1200 nm as-grown and after annealed. These XRD patterns show the presence of various phases as SnS, SnS_2 and Sn_2S_3. The intensity of the major peaks of different phases and their relationship is resumed in Table 1. As shown in table 1, $\mathbf{I_{111}}$ corresponds to the SnS phase. $\mathbf{I_{130}}$ belongs to the Sn_2S_3 phase and the $\mathbf{I_{001}}$ is the most intense peak of the SnS_2 phase, according to the diffraction profiles (JCPDS card no.39-0354, card no.23-0677 and card no.14-0619). The sample with thickness of 700 nm shows an intense peak corresponding to SnS phase at $2\theta = 31.7^{o}$ which corresponds to the (111) orientation and other peaks corresponding to the SnS_2 and Sn_2S_3 phases. After annealing, the I_{111} increases, indicating a greater crystallinity of the sample. The sample with thickness of 1200 nm shows a mixture of all phases before annealing; while after annealing, the SnS_2 phase disappears, remaining a mixture of SnS and Sn_2S_3 phases. The difference in XRD patterns of the two samples can be explained by the intensities data of the major peaks reported in Table 1. When the thickness is lower, the I_{111} is much greater than in the thicker sample, while the I_{130} is very similar in both samples. This could indicate that longer deposition time affects more disordered growth of these samples that do not show a preferential orientation.

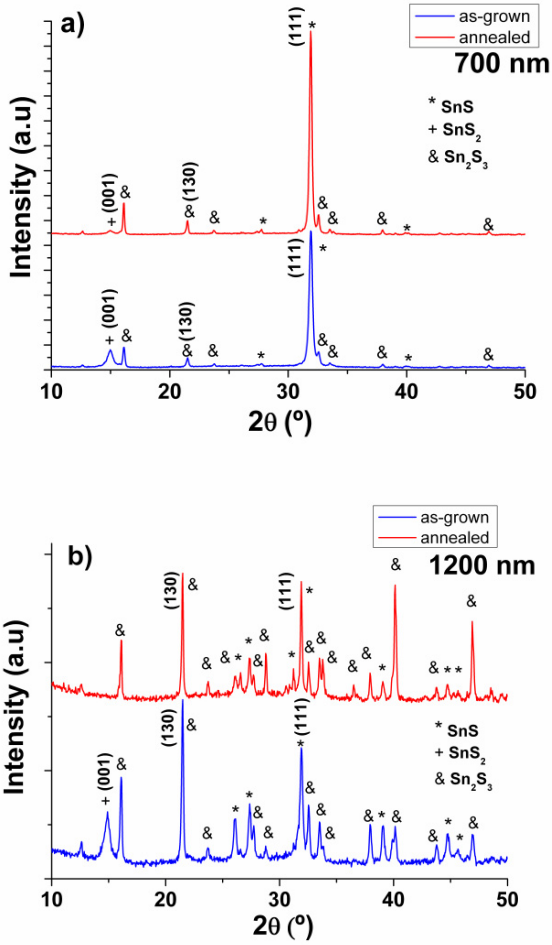

Fig. 1. XRD patterns of tin sulfide thin films with thicknesses: a) 700 nm and b) 1200 nm, obtained at 350 ºC and after annealed at 500 ºC in Ar.

Table 1. Intensity and their relationship of the major peaks for all samples obtained on bare and Mo-coated glass substrates.

Thickness (nm)	I_{111} SnS	I_{130} Sn_2S_3	I_{001} SnS_2	I_{111}/I_{001}	I_{111}/I_{130}	I_{130}/I_{001}
700 bare glass						
as-grown 350ºC	11094	850	1419	7.8	13.1	0.6
Annealed 500 ºC	16412	1196	375	43.7	12.7	3.2
1200 bare glass						
as-grown 350ºC	1116	1566	510	2.2	0.7	3.1
Annealed 500 ºC	1138	1242	0	-	0.9	-
700 Mo-coated glass						
as-grown 350ºC	178450	0	3465	51.5	-	0
Annealed 500 ºC	167736	0	3064	54.7	-	0
1200 Mo-coated glass						
as-grown 350ºC	80173	0	0	-	-	-
Annealed 500 ºC	436725	0	0	-	-	-

Figure 2 a-b shows the XRD patterns of tin sulfide thin films obtained on Mo-coated glass substrate and after annealed. According to the XRD diffractogram, the samples show an intense peak corresponding to SnS phase at 2θ =31.7º which corresponds to the (111) orientation and other peaks corresponding to the SnS_2 phase and cubic Mo phase (JCPDS 42-1120). This also occurs in SnS samples obtained by other authors on Mo-coated glass substrates [7, 24, 25]. When the sample with thickness of 1200 nm is annealed, the intensity of the main peak corresponding to the (111) orientation SnS phase considerably increases, as shown in Figure 2-b.

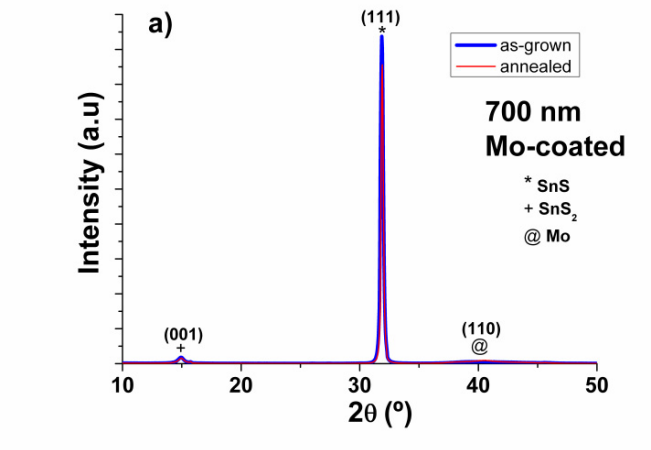

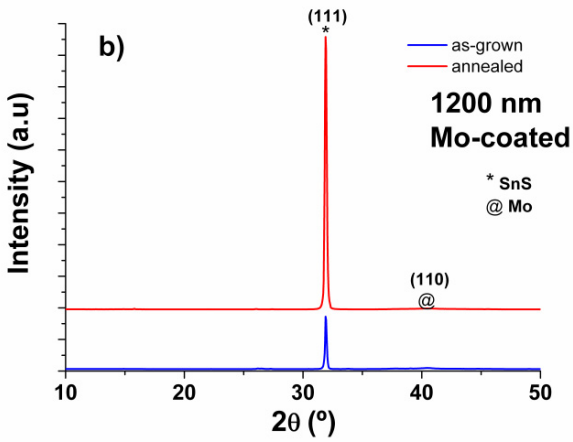

Fig. 2. XRD patterns of tin sulfide thin films on Mo-coated glass substrate with thicknesses: a) 700 nm and b) 1200 nm obtained 350ºC and after annealed at 500ºC in Ar.

Figure 3 shows an infrared thermographic image of bare glass and Mo-coated glass, within the vacuum chamber where the different samples are prepared. This is used to analyze the difference between samples on the bare glass and those obtained on Mo-coated glass. This image was performed by heating both substrates through lamps. The yellow and orange colors belong to the Mo-coated glass, while the green colors belong to the bare glass, having a temperature difference between two substrates of about 50 °C according to the temperature scale on the right of the image. This fact indicates that the samples obtained on Mo-coated glass are at a higher temperature with respect to samples obtained on bare glass, resulting therefore in a higher crystallinity of the samples and the majority presence of the SnS phase, when obtained on Mo-coated glass, as indicated us for tin sulfide thin films obtained at higher substrate temperatures on glass substrates [22].

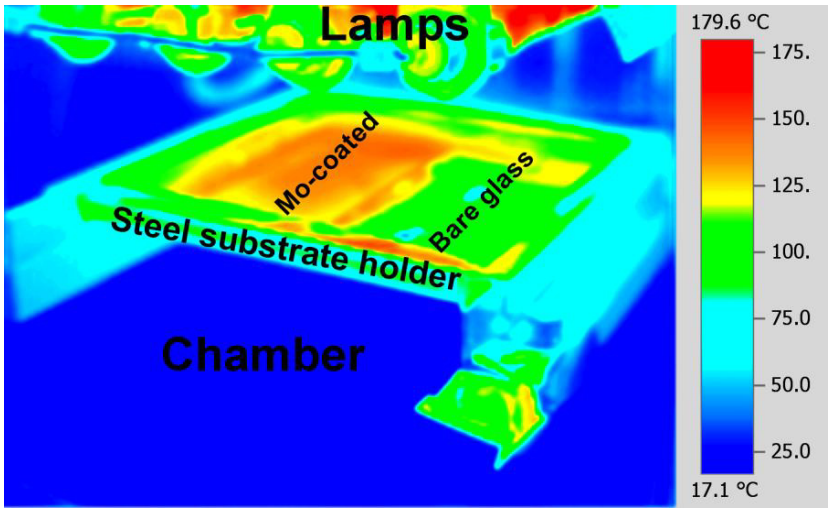

Fig. 3. Infrared thermographic image obtained for bare and Mo-coated glass substrates.

The chemical composition values are presented in Table 2. As shown in the table, the S/Sn ratio values vary from 1.0 to 1.2 for the different samples obtained on bare and Mo-coated glass substrates and after annealed. These

values of chemical composition indicate that the major phase in the structure of the obtained samples is SnS, although XRD patterns show phase mixture.

Table 2. Chemical composition measured by EDAX for the as-grown tin sulfide thin films with different thicknesses and after annealed at 500 ºC in Ar.

thickness (nm) (as-grown)	S %at	Sn %at	S/Sn	thickness (nm) (annealed 500 ºC)	S %at	Sn %at	S/Sn
700 (350ºC)	54	46	1.2	700	53	47	1.1
1200 (350ºC)	50	50	1.0	1200	51	49	1.0
700 Mo-coated (350ºC)	52	48	1.1	700 Mo-coated	55	45	1.2
1200 Mo-coated (350ºC)	51	49	1.0	1200 Mo-coated	51	49	1.0

The surface morphology has been analyzed by SEM images as those presented in figure 4 a-d. Images were obtained for samples on bare glass and Mo-coated glass substrates with thicknesses of 1200 nm to compare their morphology depending on the substrate where they are grown, before and after annealed at 500 ºC in Ar. The images show that tin sulfide thin films have homogeneous and uniform surface, with grain sizes growing when the sample is prepared on Mo-coated glass substrate and after annealing. This is related to the obtained X-ray data because this samples on Mo-coated glass and subsequent annealing shows only SnS crystalline phase with the highest (111) peak intensity.

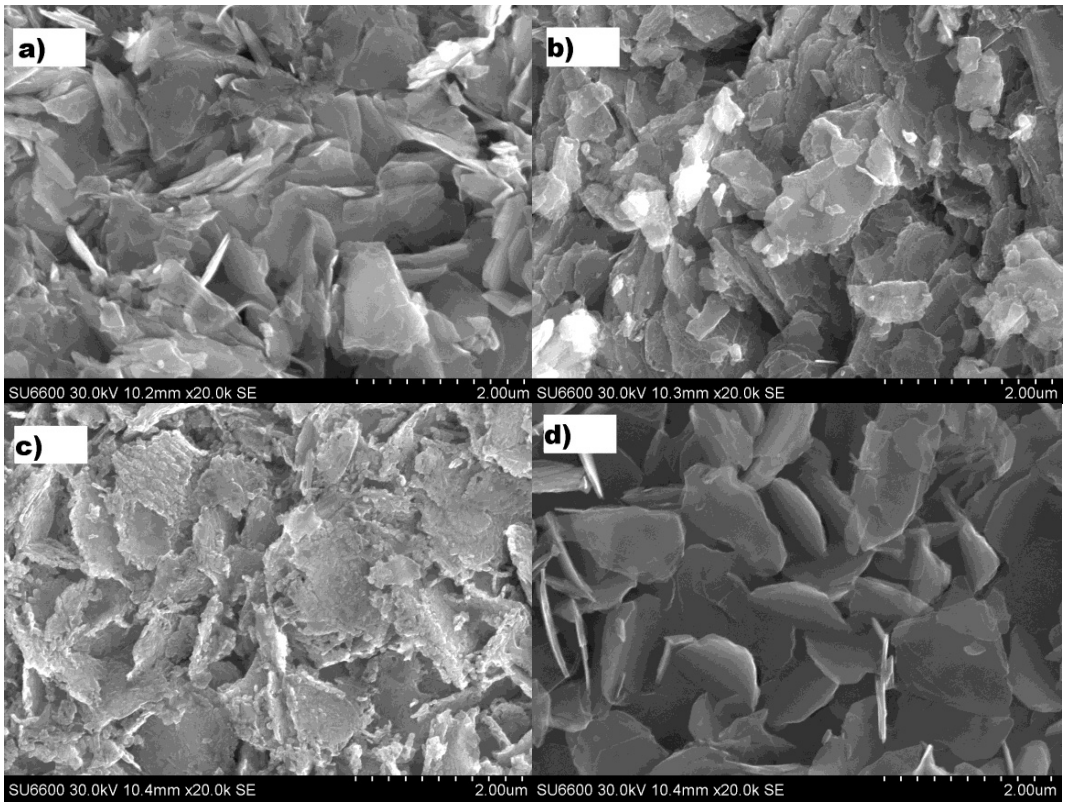

Fig. 4. SEM surface morphology of tin sulfide thin films with thicknesses: a) 1200 nm, bare glass; b) 1200 nm, bare glass, annealed; v) 1200 nm, Mo-coated glass, d) 1200 nm Mo-coated glass, annealed

All samples were characterized by their spectrum of reflectance. Figure 5 shows the reflectance for samples deposited on bare and Mo-coated glass substrate with thickness of 1200 nm. As can be seen in the spectra, the

absorption edge shifts toward shorter wavelengths after annealing. Besides maximum reflectance values are higher when samples are obtained on bare glass and after being subjected to annealing. If you look at the sample obtained on Mo-coated glass, after the annealing, the fall of the absorption edge is more pronounced, being related to the higher crystallinity of this sample appreciated in XRD patterns.

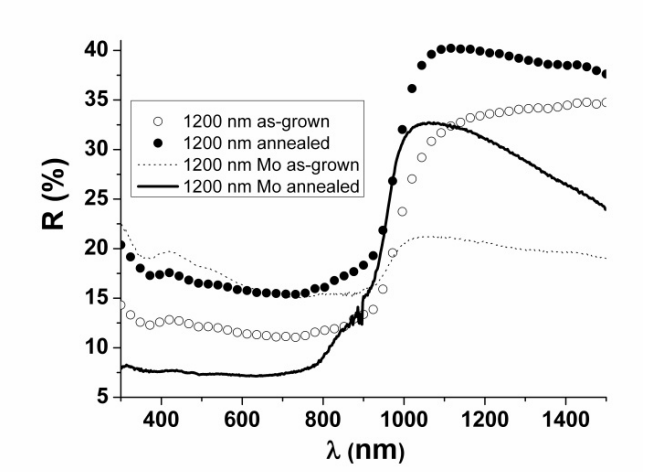

Fig. 5. Reflectance spectrum for sample with 1200 nm of thickness prepared on bare and Mo-coated glass substrates and after annealed at 500 ºC in Ar.

The absorption coefficient (α) was calculated from the transmittance and reflectance values obtained. The Eq.1 [26] allowed us to calculate α, where T is transmittance, R is reflectance, and t is the film thickness:

$$\alpha = \frac{1}{t}\ln\left\{\frac{100}{(T\% + R\%)}\right\} \tag{1}$$

Band gap energy was calculated through $(\alpha h\nu)^2$ versus $h\nu$ plot, extrapolating to the point $\alpha=0$ in the Figure 6. The figure 6 shows the band gap energy determination of samples with 1200 nm of thickness obtained on bare and Mo-coated glass substrates before annealing and after annealing. The band gap energy values of these samples before annealing are 1.14-1.17 eV. The band gap energy values increase slightly to 1.20 eV after annealing. This is related with reflectance measurements because the samples before annealing have the absorption edge to longer wavelengths, while after annealing, the absorption edge shifts slightly to shorter wavelengths. These values are very similar to those obtained by other authors for SnS thin films on glass substrate [12], and lower than those obtained by us for SnS layer [22], due to the higher thickness of these samples. These data indicate a potential use of these samples as absorbers in solar applications.

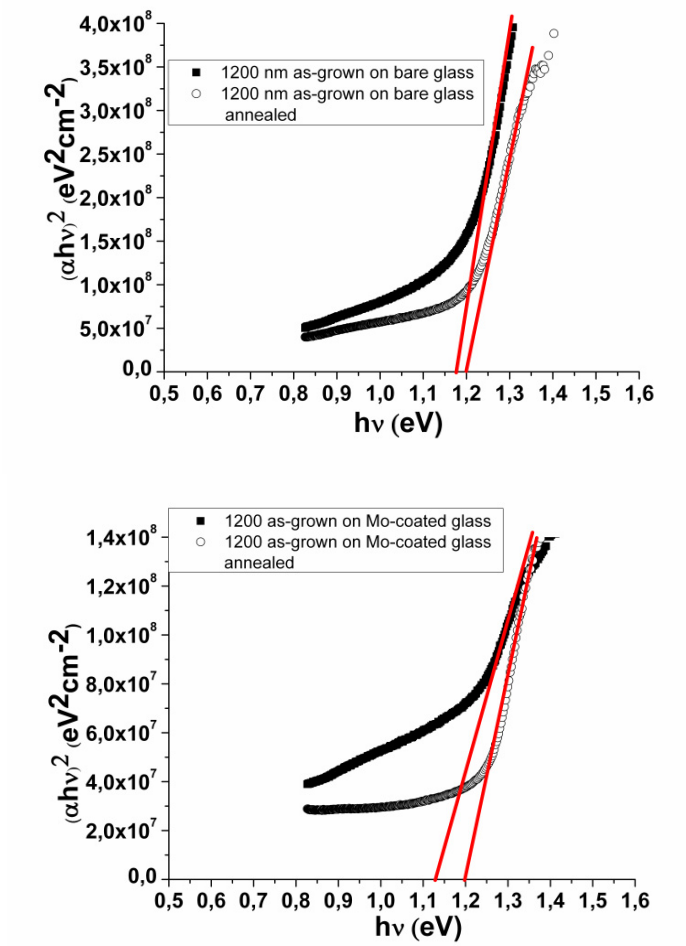

Fig. 6. Band gap determination for the sample with thickness of 1200 nm obtained on bare and Mo-coated glass substrates

4. Conclusions

Tin sulfide thin films prepared by co-evaporation have shown different properties, depending on the substrate. When samples were obtained on bare glass substrate at 350ºC, XRD patterns showed a mixture of SnS, Sn_2S_3 and SnS_2 phases, SnS_2 decreasing after post-deposition annealing at 500ºC in Ar. However, when samples were obtained on Mo-coated glass substrate, XRD patterns showed an increase in the crystallinity of the samples and the preponderance of the SnS phase, due to the higher surface temperature of Mo-coated glass substrate with respect to bare glass substrate, according to the infrared thermography. SEM images showed uniform and homogeneous surfaces with grain sizes grown when the samples were obtained on Mo-coated glass substrate and after annealing. Maximum reflectance values are influenced by the substrate and the annealing, being greater when the samples were obtained on bare glass substrate and after annealing. All samples obtained presented band gap energy between 1.14-1.20 eV, and therefore could be used as an absorber layer in photovoltaic devices.

Acknowledgements

This work has been supported by the Spanish Ministry of Economy and Competitivity through the CIEMAT.

One of the authors, V. Robles, also thanks CIEMAT for the award of a senior research fellowship.

References

[1] J. Malaquias, P. A. Fernandes, P. M. P. Salomé and A. F. da Cunha, Thin Solid Films 2011; **519**: 7416
[2] O. E. Ogah, G. Zoppi, I. Forbes and R. W. Miles, Thin Solid Films 2009 ; **517** : 2485.
[3] T. H. Sajeesh, A. R. Warrier, C. S. Kartha and K. P. Vijayakumar, Thin Solid Films 2010; **518**: 4370.
[4] L. S. Price, I. P. Parkin, A. M. E. Hardy, R. J. H. Clark, T. G. Hibbert and K. C. Molloy, Chem. Mat. 1999; **11:** 1792.
[5] A. Abou Shama and H. M. Zeyada, Optical Materials 2003; **24**: 555.
[6] S. López, A. Ortiz, Semicond. Sci. Technol. 1994; **9**: 2130.
[7] S. A. Bashkirov, V. F. Gremenok, V. A. Ivanov, V. V. Lazenka and K. Bente, Thin Solid Films 2012; **520**: 5807.
[8] M. Calixto-Rodríguez, H. Martínez, A. Sánchez-Juárez, J. Campos-Álvarez, A. Tiburcio-Silver and M. E. Calixto, Thin Solid Films 2009; **517**: 2497.
[9] N. Koteeswara Reddy, K. Ramesh, R. Ganesan, K. T. Ramakrishna Reddy, K. R. Gunasekhar and E. S. R. Gopal, Applied Physics A 2006; **83**: 133.
[10] N. G. Deshpande, A. A. Sagade, Y. G. Gudage, C. D. Lokhande and R. Sharma, Journal of Alloys and Compounds 2007; **436**: 421.
[11] S. K. Panda, A. Antonakos, E. Liarokapis, S. Bhattacharya and S. Chaudhuri, Materials Research Bulletin 2007; **42** : 576.
[12] A. Sánchez-Juárez, A. Tiburcio-Silver and A. Ortiz, Thin Solid Films 2005; **480-481**: 452.
[13] A. Sánchez-Juárez and A. Ortiz, Semicond. Sci. Technol. 2002; **17**: 931.
[14] M. Khadraoui, N. Benramdane, C. Mathieu, A. Bouzidi, R. Miloua, Z. Kebbab, K. Sahraoui and R. Desfeux, Solid State Communications 2010; **150**: 297.
[15] Z. Xu, Y. Chen, Semicond. Sci. Technol. 2012; **27**: 035007.
[16] S. Cheng, Y. Chen, C. Huang and G. Chen, Thin Solid Films 2006; **500**: 96.
[17] D. Avellaneda, M. T. S. Nair and P. K. Nair, Thin Solid Films 2009; **517:** 2500.
[18] K. Hartman, J. L. Johnson, M. I. Bertoni, D. Recht, M. J. Aziz, M. A. Scarpulla and T. Buonassisi, Thin Solid Films 2011; **519** : 7421.
[19] K. T. Ramakrishna Reddy, P. Purandhara Reddy, P. K. Datta and R. W. Miles, Thin Solid Films 2002; **403-404** : 116.
[20] O. E. Ogah, K. R. Reddy, G. Zoppi, I. Forbes and R. W. Miles, Thin Solid Films 2011; **519**: 7425.
[21] N. Sato, M. Ichimura, E. Arai and Y. Yamazaki, Solar Energy Materials and Solar Cells 2005; **85**: 153.
[22] V. Robles, J. F. Trigo, C. Guillén and J. Herrero, J. Mater. Sci. 2013; **48**: 3943.
[23] C. Cifuentes, M. Botero, E. Romero, C. Calderón and G. Gordillo, Braz. J. Phys. 2006; **36**: 1046.
[24] S. Bashkirov, V. Gremenok, V. Ivanov and V. Shevtsova, Physics of the Solid State 2012; **54**: 2497.
[25] M. Leach, K. T. R. Reddy, M. V. Reddy, J. K. Tan, D. Y. Jang and R. W. Miles, Energy Procedia 2012; **15**: 371.
[26] K. Bindu, P. K. Nair, Semicond. Sci. Technol. 2004; **19**: 1348.